

Theoretical Study of the Integral Cross Sections in the Reaction $He + H_2^+ \rightarrow HeH^+ + H$ on a Newly Revised Potential Energy Surface

Tianyun Chen, Weiping Zhang,* Haibo Ma, and Jing Cui

School of Materials Science and Engineering, Dalian University of Technology, Dalian 116024, P. R. China

Received April 30, 2010; E-mail: zhangwp@dlut.edu.cn

In the present work, dynamics information on a newly revised potential energy surface of Aquilanti et al. (*Chem. Phys. Lett.* **2009**, *469*, 26) has been presented for the $He + H_2^+ \rightarrow HeH^+ + H$ reaction. Quasiclassical trajectory (QCT) calculation has been carried out with the initial value of vibration quantum number (v) of the reaction being set from 1 to 3 and rotation quantum number (j) unchanged for zero. The results of integral cross sections are compared with both theoretical and experimental results at collision energy ranging from 0 to 2.0 eV, and all the calculated results show a reasonable agreement with experimental values. The polarized dependent differential cross section (PDDCS) was studied also, and showing that the reaction mainly display forward scattering. In addition, the vector correlation information demonstrated that the product alignment is sensitive to the vibration quantum number at collision energy of 1 eV ($=23.06\,\mathrm{kcal\,mol^{-1}}$).

The reaction $He + H_2^+ \rightarrow HeH^+ + H$ has been extensively studied in many theoretical and experimental investigations over the past three decades.[1–11] As a typical ion-molecular reaction, it was the first for which initial vibrational state selection of reactants was accomplished experimentally.[12–21] Previous studies revealed that vibrational excitation of H_2^+ enhanced the reaction cross section (σ_R) and that excitation function, which relative collision energy (E of the reactants) rise from zero at the threshold to a maximum and then declined sharply.[22–24] In recent years, there has been considerable progress in developing accurate potential energy surfaces of the reactive system.[25–28] In order to get more dynamics information, theoretical and experimental results are always compared with each other. In this letter, we performed quasiclassical trajectory (QCT) calculations to produce the integral cross sections of the reaction $He + H_2^+ \rightarrow HeH^+ + H$, and comparing them with the experimental results of Tang et al.[5] and with the QCT results of Xu et al.[7]

The new potential energy surface employed in the present calculation was constructed by Aquilanti et al.[4] at the full configuration interaction level, in order to both validate and possibly improve the previous calculated points and their fittings. From their earlier experience calculation on the PES,[2] they revised the potential energy surface which is divided into eight important regions, and described all of them with (1) 60 geometries for describing the stable intermediate HeH_2^+, (2) 105 geometries describing the insertion complex $HHeH^+$, (3) and (4) 35 geometries each for the entrance and exit channel of the reaction, (5) 29 geometries corresponding to the dissociative asymptote of the T-shape $HHeH^+$ complex, (6) 245 geometries similar to the astride of the ridge of the reaction as reported in the previous surface, (7) 755 geometries spaced on a three-body grid of hyperspherical coordinates, and (8) 247 points selected arbitrarily. All these 1511 points lie below the complete dissociation ($He + H + H^+$) energy level.

Tang et al.[5] investigated the title reaction over a broad range of reactant vibrational levels using high-resolution ultraviolet to prepare reactant ions either through excitation of autoionization resonance, or using the PFI-ESICO (pulse-field ionization-photoelectron-secondary ion coincidence) approach. They measured the integral cross sections for $v = 0$–3 (v: vibration quantum number) with high signal-to-noise using a guided-ion beam, and PFI-ESICO cross sections are reported for $v = 1$–15 and $v = 0$–12 at center-of-mass collision energies of 0.6 and 3.1 eV, respectively. In their experiment, they showed some discrepancies between the reported cross sections and a number of quantum scattering studies used the same ab initial potential energy surface provided by Palmieri et al.[2] The translational energy dependence measurements for $v = 0$–3 are in good agreement with most of their previous experiments. They also did some significant QCT calculations on the potential energy surface constructed by Aquilanti and coworkers.[2] They calculated cross sections for $v \geq 0$ at low total energies ($\leq$1 eV) were significantly higher than the measured values, the overestimate of the resonances in the theoretical work may attribute to some inaccuracies of the potential energy surface. At $E = 0.6$ eV, and for reactant initial states in $j = 1$ and $v = 1$–15 (j: rotation quantum number), and at higher reactant levels of v, the experimental and QCT results of cross sections agree within the experiments uncertainties, but the cross section declined above $v = 11$. And with E_T increased to 3.1 eV, the PFI-ESICO measurements agree very well with the QCT results. Chu et al. performed time-dependent wave packet calculations for the $He + H_2^+ \rightarrow HeH^+ + H$ reaction on the same potential energy surface of Aquilanti and coworkers.[29–31] Comparison between the quantum scattering calculations with and without Coriolis couplings in their study first revealed an important role of Coriolis coupling effect in performing an accurate quantum scattering calculation for the title reaction.

Published on the web October 21, 2010; doi:10.1246/bcsj.20100127

Recently, Han[32–40] and co-workers had developed a QCT method to calculate the trajectory of heavy heavy–light, light light–light, heavy light–light, and light heavy–light mass combination reactions on attractive and repulsive potential energy surfaces to study the dependence relation of product rotational alignment, polarized dependent differential cross section, and other stereodynamics information on different collision energies for triatomic reaction A + BC.[25,26,41–43] Xu et al. carried out several QCT studies on the $He + H_2^+ \rightarrow HeH^+ + H$ reaction using the XL PES.[7–9] They computed the reaction cross sections and compared with Tang's experimental results for $\boldsymbol{v} = 0$–3. Their results show obviously vibrational enhancement, and are in good agreement with experiment results.[7] They also studied the stereodynamics and the isotopic effect of the reaction.[9]

In the present work, we calculated the integral cross section of the reaction and compared them with the experimental results of Tang et al.[5] and the QCT results of Xu et al.[7] And the angular distributions of $P(\theta_r)$, $P(\phi_r)$ the polarized dependent differential cross sections (PDDCSs) of the reaction for different values of $\boldsymbol{v}$ at 1.0 eV have been calculated also. With the vibration quantum number being initially set for $\boldsymbol{v} = 1$–3 and $\boldsymbol{j} = 0$, 50000 trajectories are run, and the integration step size is chosen as 0.1 fs.

Theoretical

The integral cross section is defined as

$$\sigma_R = \pi {b_{max}}^2 (N_r/N) \tag{1}$$

N_r is the reactive trajectories of the two channels and N is the total trajectories we have set, and the sampling error is

$$\sigma = \sqrt{(N - N_r)/NN_r} \times 100\ (\%) \tag{2}$$

The fully correlated center-of-mass angular distribution is written as the sum

$$P(\cos\theta, \cos\theta_r, \phi_r) = \frac{1}{4\pi} \sum_{k=0}^{\infty} \sum_{q=-k}^{k} (2k+1) \times \frac{2\pi}{\sigma} \frac{d\sigma_{kq}}{d\omega} C_{kq}(\theta_r, \phi_r) \tag{3}$$

Where $\omega = \theta, \phi$ and $\omega_r = \theta_r, \phi_r$ refers to the coordinates of the unit vectors $\boldsymbol{k'}$ and $\boldsymbol{j'}$ along the directions of the product relative velocity and rotational angular momentum vectors in the CM frame, respectively. $\frac{1}{\sigma}\frac{d\sigma_{kq}}{d\omega}$ is the generalized PDDCSs.[32,44–46]

The PDDCSs are written as follow.

$$\frac{2\pi}{\sigma}\frac{d\sigma_{k0}}{d\omega} = 0 \tag{4}$$

(when k is odd)

$$\frac{2\pi}{\sigma}\frac{d\sigma_{kq+}}{d\omega} = \frac{2\pi}{\sigma}\frac{d\sigma_{kq}}{d\omega} + \frac{2\pi}{\sigma}\frac{d\sigma_{k-q}}{d\omega} = 0 \tag{5}$$

(when k is even, q is odd or k is odd q is even)

$$\frac{2\pi}{\sigma}\frac{d\sigma_{kq-}}{d\omega} = \frac{2\pi}{\sigma}\frac{d\sigma_{kq}}{d\omega} - \frac{2\pi}{\sigma}\frac{d\sigma_{k-q}}{d\omega} = 0 \tag{6}$$

(when k is even, q is odd or k is odd q is even)

We can also summarize these as

$$\frac{2\pi}{\sigma}\frac{d\sigma_{kq\pm}}{d\omega} = \sum_{k_1} \frac{[k_1]}{4\pi} S^{k_1}_{kq\pm} C_{k_1 - q}(\theta, 0) \tag{7}$$

And $S^{k_1}_{q\pm}$ was expressed as

$$S^{k_1}_{kq\pm} = \langle c_{k_1 q}(\theta, 0) c_{kq}(\theta_r, 0)[(-1)^q e^{iaxq\phi_r} \pm e^{-iaxq\phi_r}] \rangle \tag{8}$$

Double vector correlations ($\boldsymbol{k}$–$\boldsymbol{j'}$, $\boldsymbol{k}$–$\boldsymbol{k'}$, or $\boldsymbol{k'}$–$\boldsymbol{j'}$) can be expanded into a series of Legendre polynomials. The $P(\theta_r)$ distribution corresponding to the $\boldsymbol{k}$–$\boldsymbol{j'}$ correlation is written as[33–37,47]

$$P(\theta_r) = \frac{1}{2} \sum_k [k] a_0^k P_k(\cos\theta_r) \tag{9}$$

The a_0^k coefficients (polarization parameters) are given by

$$a_0^k = P_k(\cos\theta_r) \tag{10}$$

The brackets represent an average over all the reactive trajectories. The dihedral angular distribution of the $\boldsymbol{k}$–$\boldsymbol{k'}$–$\boldsymbol{j'}$ triple vectors correlation is characterized by the angle $P(\phi_r)$. The distribution of the dihedral angular discussion $P(\phi_r)$ could be expanded as a Fourier series[38–43]

$$P(\phi_r) = \frac{1}{2\pi}\left(1 + \sum_{n(\text{even})\geq 2} a_n \cos n\phi_r + \sum_{n(\text{odd})\geq 1} b_n \sin\phi_r\right) \tag{11}$$

With a_n and b_n given by

$$a_n = 2\langle \cos n\phi_r \rangle \tag{12}$$

$$b_n = 2\langle \sin n\phi_r \rangle \tag{13}$$

In the work, when $P(\phi_r)$ is expended up to $n = 24$ can get convergence results.

Results and Discussion

50000 trajectories are run for each value of $\boldsymbol{v}$ over a range of collision energy on the revised potential energy surface of Aquilanti.[4] For $\boldsymbol{v} = 0$, the calculations are not in accord with experiment results, so we calculated the reaction cross section with initial vibrational number $\boldsymbol{v} = 1$–3 and initial rotation number $\boldsymbol{j} = 0$, the collision energy from 0 to 2.0 eV, and the energy grid is 0.1 eV.

Figure 1 shows the cross section for $\boldsymbol{v} = 1, \boldsymbol{j} = 0$. Overall, the integral reaction cross sections computed on the revised surface agree very well with Xu's QCT results and reasonable agreement with experiment results of Tang. In detail, for $\boldsymbol{v} = 1, \boldsymbol{j} = 0$ case, and over the range of collision energy, comparison with those published results show agreement in the overall behavior. From Figure 1, we can obtain that the maximum value of the cross section at about 0.8 eV. It is clearly that our results agree very well with QCT results of Xu and experimental results of Tang at energy points $E \leq 0.6$ eV and $E \geq 1.5$ eV. But between these two energy points, it has obviously discrepancy in that all of the theoretical studies are larger than experimental results. We had known that the threshold energy of this reaction is about 0.4 eV which was smaller than Tang's experimental result 0.512 eV, and the GIB work of Achtenhagen[11] measured it above 1 eV, our result lies between them.

It can be clearly seen from Figure 2 that for the cross section of $\boldsymbol{v} = 2$, the experimental data of Tang et al. is slightly lower than the theoretical data near the threshold. But the trend of all the results agreed very well. Comparison of our QCT results with those of Tang et al. and Xu et al. shows a reasonable agreement, and all of the simulation results are larger than the experimental result. This phenomenon may be caused by the differences of potential energy surfaces.

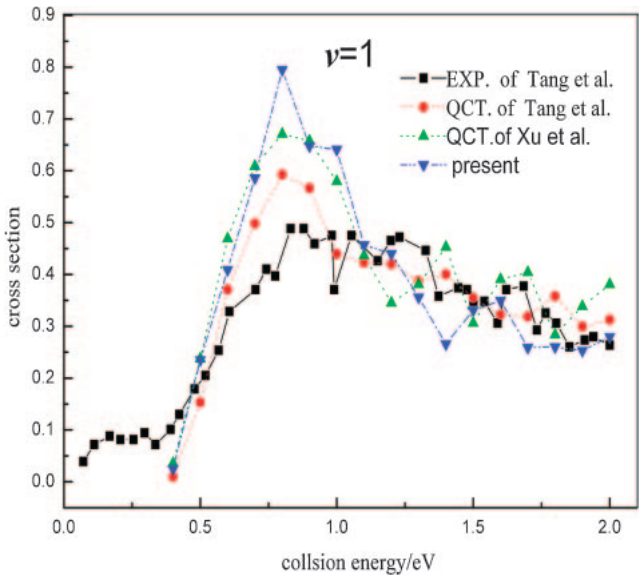

Figure 1. Comparison of the present QCT results with the QCT results of Xu, QCT and experiment results of Tang et al. at $\boldsymbol{v} = 1$.

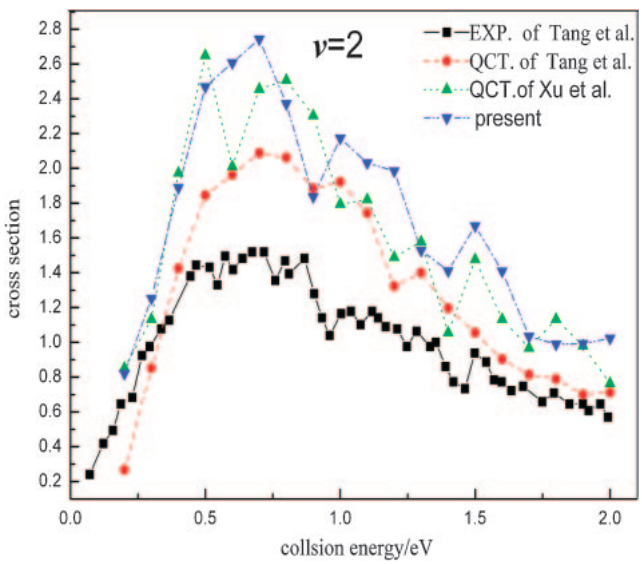

Figure 2. Comparison of the present QCT results with the QCT results of Xu, QCT and experiment results of Tang et al. at $\boldsymbol{v} = 2$.

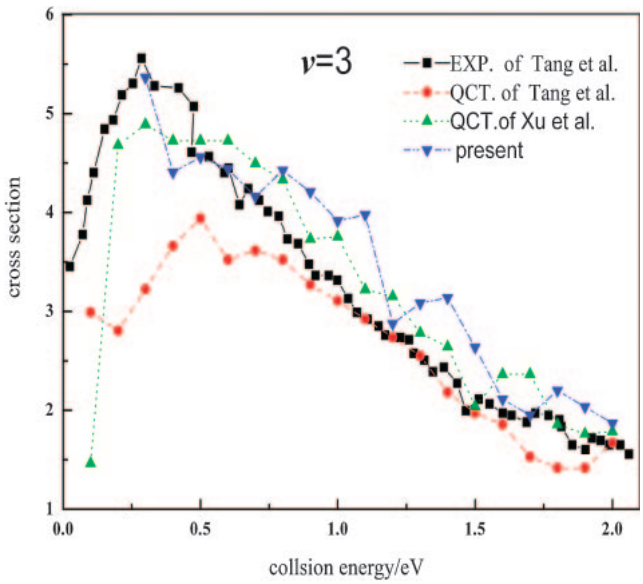

Figure 3. Comparison of ours results with the QCT results of Xu, QCT and experiment results of Tang et al. at $\boldsymbol{v} = 3$.

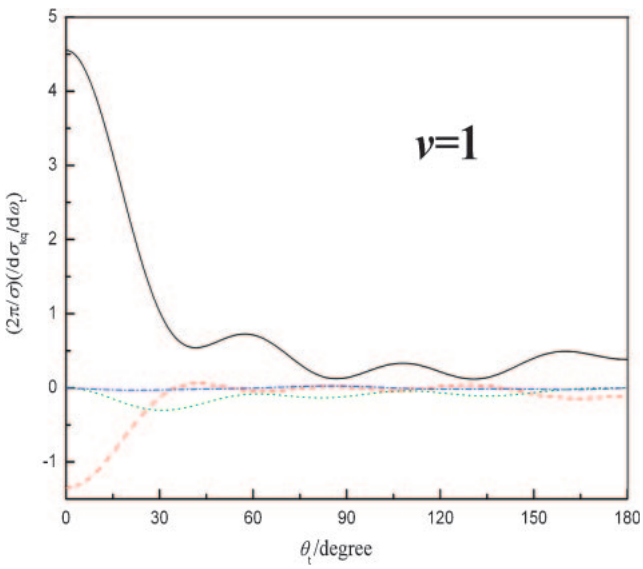

Figure 4. Quasiclassical PDDCSs for the $He + H_2^+ \rightarrow HeH^+ + H$ reaction on the revised potential energy surface for $\boldsymbol{v} = 1$. $(2\pi/\sigma)(d\sigma_{00}/d\omega_t)$ solid line, $(2\pi/\sigma)(d\sigma_{20}/d\omega_t)$ dash line, $(2\pi/\sigma)(d\sigma_{22+}/d\omega_t)$ dot line, and $(2\pi/\sigma)(d\sigma_{21-}/d\omega_t)$ dash dot line.

For initial vibrational state of $\boldsymbol{v} = 3$ in Figure 3, it can be seen that when collision energy is smaller than 0.7 eV and larger than 1.6 eV, our results agree better with experimental results than Xu's and Tang's QCT. And Tang's QCT result is smaller than the experimental result, ours and Xu's are larger than experimental results. But between the two collision energies, all of the theoretical studies have some discrepancy with experimentals, ours and Xu's results are larger than experimental, and Tang's results agree very well in this region.

Probably, the differences between the present results and the previous theoretical results, generating on three different potential energy surfaces are due to the different interaction region of potential well. The reaction is directly determined by the position and the depth of the potential well. The PES revised by Aquilanti et al. has different optimized distances and the dissociation energies from the other two potential energy surfaces, which has been describe in Ref. 4. Maybe all of these are responsible for the discrepancy of the cross sections. Just like Xu had explained, the sample error suggests that error of the QCT calculation is larger at lower reaction probability, probably due to that at low value of $\boldsymbol{v}$ the potential energy surface is less accuracy.

In order to obtain more information on the potential energy surface, we computed the PDDCSs of this reaction. The QCT

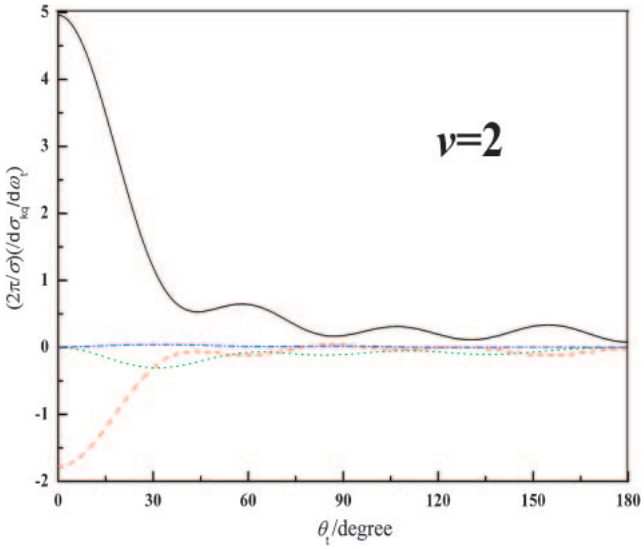

Figure 5. Quasiclassical PDDCSs for the $He + H_2^+ \rightarrow HeH^+ + H$ reaction on the revised potential energy surface for $v = 2$. $(2\pi/\sigma)(d\sigma_{00}/d\omega_t)$ solid line, $(2\pi/\sigma)(d\sigma_{20}/d\omega_t)$ dash line, $(2\pi/\sigma)(d\sigma_{22+}/d\omega_t)$ dot line, and $(2\pi/\sigma)(d\sigma_{21-}/d\omega_t)$ dash dot line.

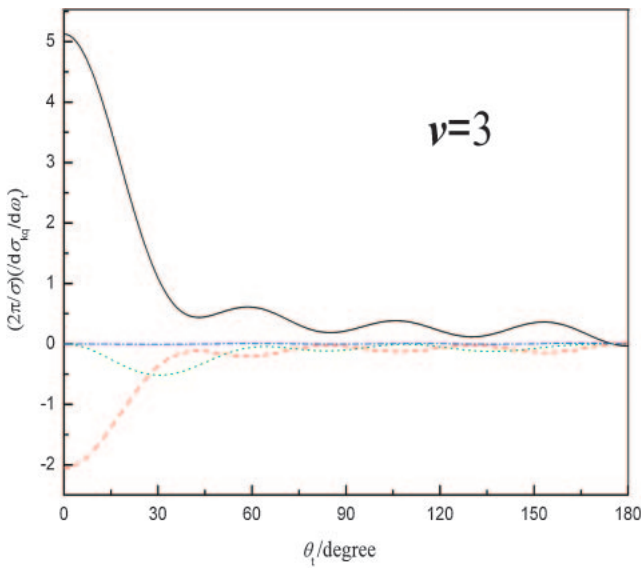

Figure 6. Quasiclassical PDDCSs for the $He + H_2^+ \rightarrow HeH^+ + H$ reaction on the revised potential energy surface for $v = 3$. $(2\pi/\sigma)(d\sigma_{00}/d\omega_t)$ solid line, $(2\pi/\sigma)(d\sigma_{20}/d\omega_t)$ dash line, $(2\pi/\sigma)(d\sigma_{22+}/d\omega_t)$ dot line, and $(2\pi/\sigma)(d\sigma_{21-}/d\omega_t)$ dash dot line.

results of product HeH^+ for different value of v for the reaction of $He + H_2^+ \rightarrow HeH^+ + H$ calculated at the collision energy of 1 eV (=23.06 kcal mol^{-1}) are depicted in Figure 4, Figure 5, and Figure 6. The PDDCS describes the correlation of k–k'–j' and scattering direction of the product molecule. The PDDCS $(2\pi/\sigma)(d\sigma_{00}/d\omega_t)$, which is simply the differential cross-section (DCS), only describe the k–k' correlation or the scattering direction of the product and is not associated with the orientation and alignment of the product rotational angular momentum vector. It is obvious that for different values of v,

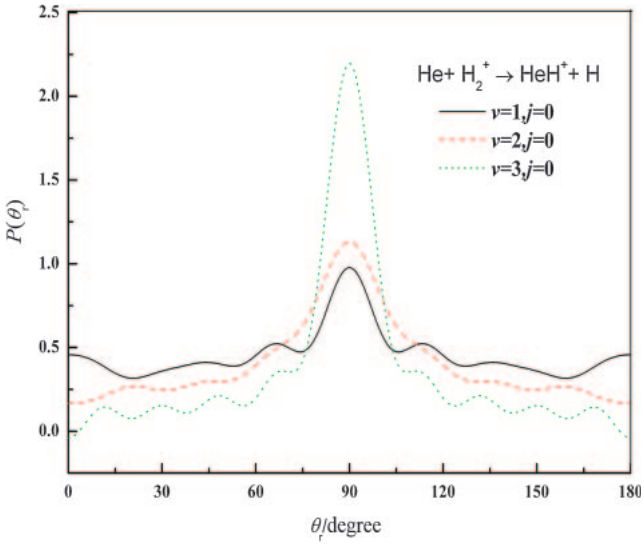

Figure 7. The distribution of $P(\theta_r)$ reflecting the k–j' correlation for $He + H_2^+ \rightarrow HeH^+ + H$ ($v = 1$–3, $j = 0$) reactions.

the product molecules are mainly scattered forward, and backward scattering is weaker. It can be clearly seen from the three figure that the value of $(2\pi/\sigma)(d\sigma_{00}/d\omega_t)$ is increased when the value of v changes from 1 to 3, implying that the forward scattering is becoming stronger and backward scattering becoming weaker.

The PDDCS $(2\pi/\sigma)(d\sigma_{20}/d\omega_t)$ is the expectation value of the second Legendre moment, whose value shows a trend opposite to $(2\pi/\sigma)(d\sigma_{00}/d\omega_t)$, indicating that j' is strongly aligned perpendicular to k. This phenomenon is due to $(2\pi/\sigma)(d\sigma_{20}/d\omega_t)$ being related to the alignment momenta $\langle P_2(\cos\theta)\rangle$. The detailed discussion of the product rotation alignment effect will be the topic of our next work. At the extremes of forward and backward scattering, the PDDCSs with $q \neq 0$ are necessarily zero,[40] which can be seen from Figures. The PDDCS $(2\pi/\sigma)(d\sigma_{22+}/d\omega_t)$ strongly depends on the scattering angle. As we can see from the Figures, all the values of $(2\pi/\sigma)(d\sigma_{22+}/d\omega_t)$ for the title reaction are negative for all scattering angles, reveals that noticeable preference for an alignment of j' along to the y axis as opposed to the x axis. The distribution of $(2\pi/\sigma)(d\sigma_{21-}/d\omega_t)$ which is related to $(\sin 2\theta_r, \cos 2\phi_r)$ is closing zero on the surface and almost a straight line. That is to say $(2\pi/\sigma)(d\sigma_{21-}/d\omega_t)$ obviously isotropic and almost independent of surface.

Figure 7 is about the distribution of $P(\theta_r)$, it describes the k–j' vector correlation with $k \cdot j' = \cos\theta_r$. It can be clearly see that there are three peaks at $\theta_r = 90°$ and all of them are symmetric with respect to 90°, indicating that the product angular momentum j' tends to perpendicular to k. As the value of v increases, there is a contraction in the calculated $P(\theta_r)$ distributions with the peak moving upward, thus suggest that the product alignment becomes stronger at high values of v.

The dihedral angle distributions of the k–k'–j' correlation is expressed as $P(\phi_r)$ it can provide stereodynamic information on both product alignment and product orientation (Figure 8). The distributions of $P(\phi_r)$ tend to be asymmetric about $\phi_r = 180°$, directly reflecting the strong polarization of angular momentum

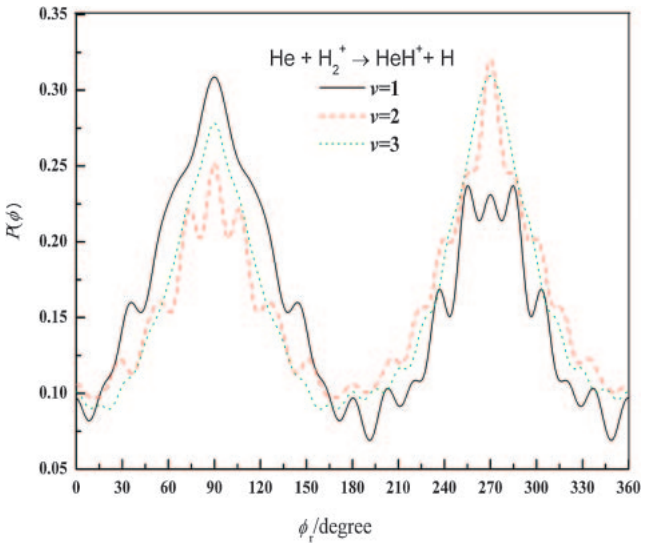

Figure 8. Dihedral angle distribution of $\boldsymbol{j}'$, $P(\phi_r)$ with respect to the $\boldsymbol{k}$–$\boldsymbol{k}'$ plane.

for the reaction. On the scattering plane of $\boldsymbol{k}$–$\boldsymbol{k}'$, with one small (or no peak) and one large peak appearing at/around $\phi_r = 90°$ and $\phi_r = 270°$ respectively. This feature shows that all product molecules tend to point to the negative direction of $\boldsymbol{y}$ axis. But the peak at $\phi_r = 90°$ is not equal to $\phi_r = 270°$, this phenomenon shows that the product rotation angular momentum vector $\boldsymbol{j}'$ is not only aligned but also oriented along the $\boldsymbol{y}$ axis. Comparing the $P(\phi_r)$ distribution generated for the three value of $\boldsymbol{v}$, we see that products formed for $\boldsymbol{v} = 3$ have shown the strongest alignment and orientation, next is $\boldsymbol{v} = 2$ while those for $\boldsymbol{v} = 1$ is the least. This indicates that with increasing the value of $\boldsymbol{v}$, the product alignment and orientation become stronger.

Conclusion

In this work, QCT calculation of the $He + H_2^+ \rightarrow HeH^+ + H$ reaction on a new potential energy surface revised by Aquilanti et al.[4] were carried out for the first time. We calculate the integral cross section and set the initial vibration quantum number from 1 to 3. We also compare the calculated QCT results with the experimental results of Tang et al.[5] and the QCT values of Xu et al.[7] From the comparison, the $\boldsymbol{v} = 1$ and $\boldsymbol{v} = 3$ results is in good agreement with experiment results when collision energy is smaller than 0.6 eV and larger than 1.5 eV. But for $\boldsymbol{v} = 2$, all of the QCT results are larger than experimental results. In a word, though there are some discrepancies, the whole trend corresponds very well with experiments, and the potential energy surface is very accurate, especially for high collision energy. Also, we do some stereodynamics computation for the polarized dependent differential cross sections (PDDCSs) for $\boldsymbol{v} = 1$ to $\boldsymbol{v} = 3$, and collision energy is chosen to be 1 eV. From the results we can see that the reaction $He + H_2^+ \rightarrow HeH^+ + H$ mainly show forward scattering, and forward scattering become stronger with increasing the value of $\boldsymbol{v}$. Comparing the distributions of $P(\theta_r)$ and $P(\phi_r)$ of the title reaction for initial vibrational states $\boldsymbol{v} = 1$–3, $\boldsymbol{j} = 0$, it is found that that with increasing the value of $\boldsymbol{v}$, not only the product orientation becomes stronger, but also its alignment become stronger too.

The authors are very grateful to Professor V. Aquilanti and C. N. Ramachandran for providing the new potential energy surfaces. The authors also thank Professor K. Han for providing the QCT code of stereodynamics.

References

1 T. Zhang, X.-M. Qian, X. N. Tang, C. Y. Ng, Y. Chiu, D. J. Levandier, J. S. Miller, R. A. Dressler, *J. Chem. Phys.* **2003**, *119*, 10175.

2 P. Palmieri, C. Puzzarini, V. Aquilanti, G. Capecchi, S. Cavalli, D. D. Fazio, A. Aguilar, X. Giménez, J. M. Lucas, *Mol. Phys.* **2000**, *98*, 1835.

3 V. Aquilanti, G. Capecchi, S. Cavalli, D. De Fazio, P. Palmieri, C. Puzzarini, A. Aguilar, X. Giménez, J. M. Lucas, *Chem. Phys. Lett.* **2000**, *318*, 619.

4 C. N. Ramachandran, D. D. Fazio, S. Cavalli, F. Tarantelli, V. Aquilanti, *Chem. Phys. Lett.* **2009**, *469*, 26.

5 X. N. Tang, H. Xu, T. Zhang, Y. Hou, C. Chang, C. Y. Ng, Y. Chiu, R. A. Dressler, D. J. Levandier, *J. Chem. Phys.* **2005**, *122*, 164301.

6 B. Maiti, C. Kalyanaraman, A. N. Panda, N. Sathyamurthy, *J. Chem. Phys.* **2002**, *117*, 9719.

7 W. W. Xu, X. G. Liu, S. X. Luan, Q. G. Zhang, P. Zhang, *Chem. Phys. Lett.* **2008**, *464*, 92.

8 G.-J. Zhao, K.-L. Han, *Biophys. J.* **2008**, *94*, 38.

9 W. W. Xu, X. G. Liu, S. X. Luan, Q. G. Zhang, *Chem. Phys.* **2009**, *355*, 21.

10 A. K. Tiwari, S. Kolakkandy, N. Sathyamurthy, *J. Phys. Chem. A* **2009**, *113*, 9568.

11 M. Achtenhagen, M. Schweizer, D. Gerlich, private communication; S. Kumar, N. Sathyamurthy, K. C. Bhalla, *J. Chem. Phys.* **1993**, *98*, 4680.

12 N. Balakrishnan, N. Sathyamurthy, *Chem. Phys. Lett.* **1995**, *240*, 119.

13 G.-J. Zhao, K.-L. Han, Y.-B. Lei, Y. Dou, *J. Chem. Phys.* **2007**, *127*, 094307.

14 A. K. Tiwari, N. Sathyamurthy, *J. Phys. Chem. A* **2006**, *110*, 11200.

15 G.-J. Zhao, Y.-H. Liu, K.-L. Han, Y. Dou, *Chem. Phys. Lett.* **2008**, *453*, 29.

16 B. Maiti, N. Sathyamurthy, *Chem. Phys. Lett.* **2001**, *345*, 461.

17 X. Tang, C. Houchins, K.-C. Lau, C. Y. Ng, R. A. Dressler, Y.-H. Chiu, T.-S. Chu, K.-L. Han, *J. Chem. Phys.* **2007**, *127*, 164318.

18 X. Qian, T. Zhang, Y. Chiu, D. J. Levandier, J. S. Miller, R. A. Dressler, C. Y. Ng, *J. Chem. Phys.* **2003**, *118*, 2455.

19 X. Qian, T. Zhang, C. Chang, P. Wang, C. Y. Ng, Y. Chiu, D. J. Levandier, J. S. Miller, R. A. Dressler, T. Baer, D. S. Peterka, *Rev. Sci. Instrum.* **2003**, *74*, 4096.

20 P. J. Brown, E. F. Hayes, *J. Chem. Phys.* **1971**, *55*, 922.

21 P. J. Kuntz, *Chem. Phys. Lett.* **1972**, *16*, 581.

22 D. R. McLaughlin, D. L. Thompson, *J. Chem. Phys.* **1979**, *70*, 2748.

23 W. A. Chupka, M. E. Russell, K. Refaey, *J. Chem. Phys.* **1968**, *48*, 1518.

24 J. Hu, K.-L. Han, G.-Z. He, *Phys. Rev. Lett.* **2005**, *95*, 123001.

25 T. Turner, O. Dutuit, Y. T. Lee, *J. Chem. Phys.* **1984**, *81*, 3475.

26 W. A. Chupka, in *Ion-Molecule Reactions*, ed. by J. L.

Franklin, Plenum, New York, **1972**, Vol. 1, Chap. 3, p. 72.
27 T.-S. Chu, Y. Zhang, K.-L. Han, *Int. Rev. Phys. Chem.* **2006**, *25*, 201.
28 S. Kumar, H. Kapoor, N. Sathyamurthy, *Chem. Phys. Lett.* **1998**, *289*, 361.
29 T.-S. Chu, K.-L. Han, *Phys. Chem. Chem. Phys.* **2008**, *10*, 2431.
30 T.-S. Chu, R.-F. Lu, K.-L. Han, X.-N. Tang, H.-F. Xu, C. Y. Ng, *J. Chem. Phys.* **2005**, *122*, 244322.
31 T.-S. Chu, K.-L. Han, *J. Phys. Chem. A* **2005**, *109*, 2050.
32 K.-L. Han, G.-Z. He, N.-Q. Lou, *J. Chem. Phys.* **1996**, *105*, 8699.
33 H. Zhang, R.-S. Zhu, G.-J. Wang, K.-L. Han, G.-Z. He, N.-Q. Lou, *J. Chem. Phys.* **1999**, *110*, 2922.
34 G.-J. Zhao, J.-Y. Liu, L.-C. Zhou, K.-L. Han, *J. Phys. Chem. B* **2007**, *111*, 8940.
35 M.-L. Wang, K.-L. Han, G.-Z. He, *J. Chem. Phys.* **1998**, *109*, 5446.
36 G.-J. Zhao, K.-L. Han, *J. Comput. Chem.* **2008**, *29*, 2010.
37 Y. Zhang, T.-X. Xie, K.-L. Han, *J. Phys. Chem. A* **2003**, *107*, 10893.
38 T.-S. Chu, X. Zhang, K.-L. Han, *J. Chem. Phys.* **2005**, *122*, 214301.
39 G.-J. Zhao, K.-L. Han, *J. Chem. Phys.* **2007**, *127*, 024306.
40 M.-L. Wang, K.-L. Han, G.-Z. He, *J. Phys. Chem. A* **1998**, *102*, 10204.
41 M. Brouard, H. M. Lambert, S. P. Rayner, J. P. Simons, *Mol. Phys.* **1996**, *89*, 403.
42 N. E. Shafer-Ray, A. J. Orr-Ewing, R. N. Zare, *J. Phys. Chem.* **1995**, *99*, 7591.
43 M. P. D. Miranda, D. C. Clary, J. F. Castillo, D. E. Manolopoulos, *J. Chem. Phys.* **1998**, *108*, 3142.
44 T.-X. Xie, Y. Zhang, M.-Y. Zhao, K.-L. Han, *Phys. Chem. Chem. Phys.* **2003**, *5*, 2034.
45 G.-J. Zhao, K.-L. Han, *ChemPhysChem* **2008**, *9*, 1842.
46 G.-J. Zhao, K.-L. Han, *J. Phys. Chem. A* **2007**, *111*, 2469.
47 J. T. Muckerman, *J. Chem. Phys.* **1971**, *54*, 1155.